Progress Toward An Effective Field Theory Analysis of the LUX WIMP Search

Nicole A. Larsen
Yale University
INT Workshop
9 December 2014

On behalf of the LUX Collaboration

Xenon as a Direct Detection Target

- High density (3 g/cm^3) and high atomic mass (A = 131 g/mol)
- Scintillates brightly in the near-UV (178 nm) with fast (ns) response time
- Excellent ionization threshold and long electron drift lengths (~1 m)
- High abundance of odd isotopes => spin-dependent sensitivity.

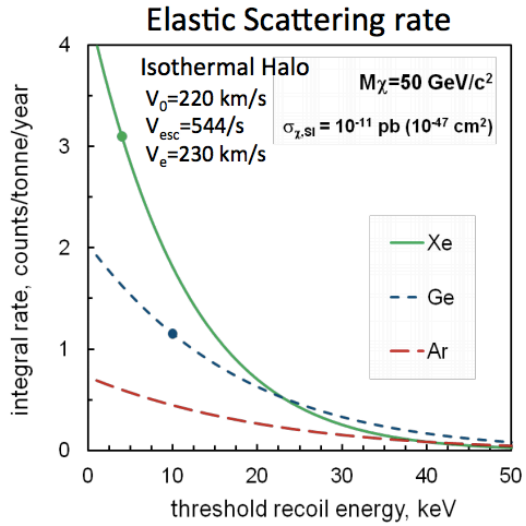

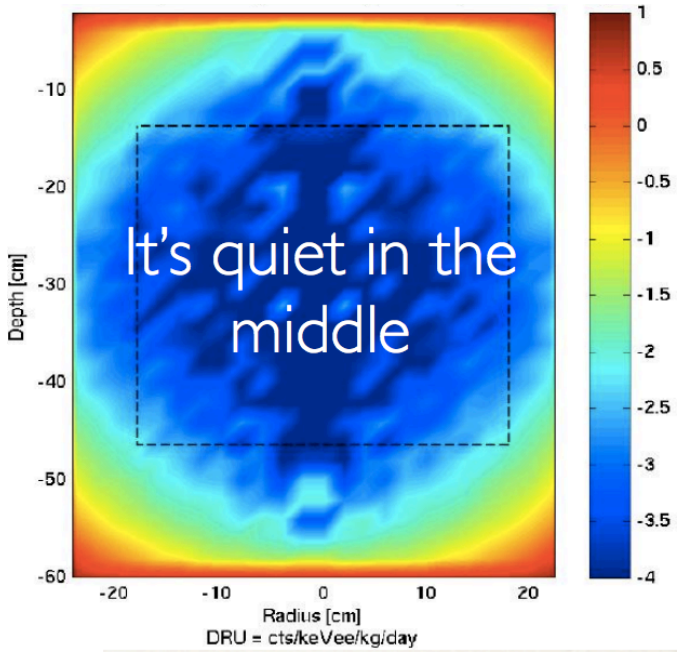

- No long-lived intrinsic backgrounds
- Scalable to multi-ton size
- Self-shielding possible with 3D reconstruction

Dual-Phase TPCs: Principle of Operation

- **The target is cooled to condensation point => liquid topped by a thin layer of gas.**
- **An incident particle excites/ionizes a target atom, which emits primary scintillation ("S1") light.**
- **Ionization electrons produced are drifted upwards by an applied electric field and extracted into the gas phase, where they are accelerated rapidly and caused to scintillate again ("proportional" or "S2" light).**

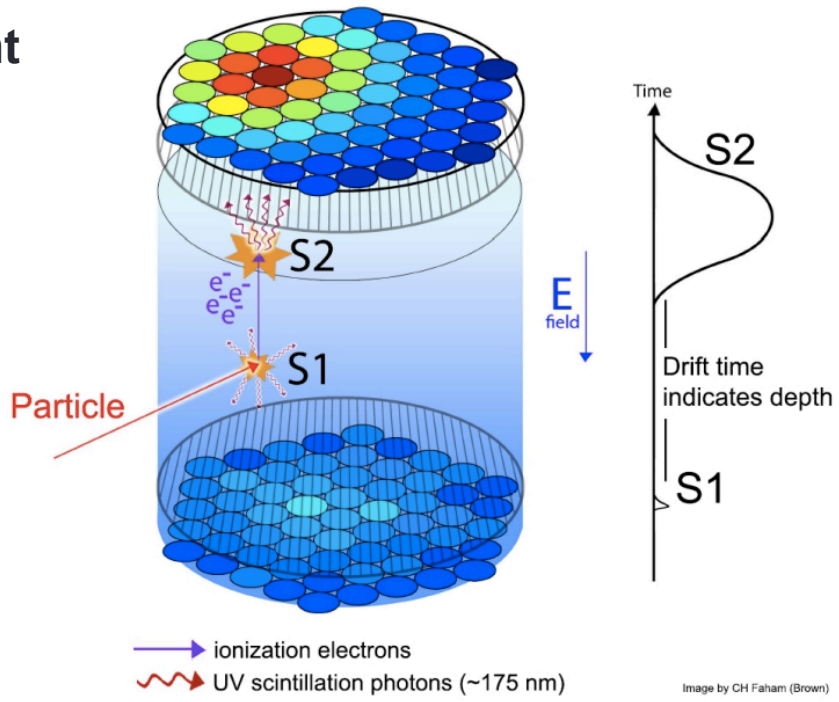

3D imaging possible:

Timing between the S1 and S2 pulses yields z-position.

PMT hit patterns yield xy-position.

ER/NR discrimination possible:

Nuclear recoils produce dense tracks

Electron recoils produce less-dense tracks

=> $(S2/S1)_{\gamma}$ >> $(S2/S1)_{neutron}$

A Typical Event: 1.5 keV Gamma

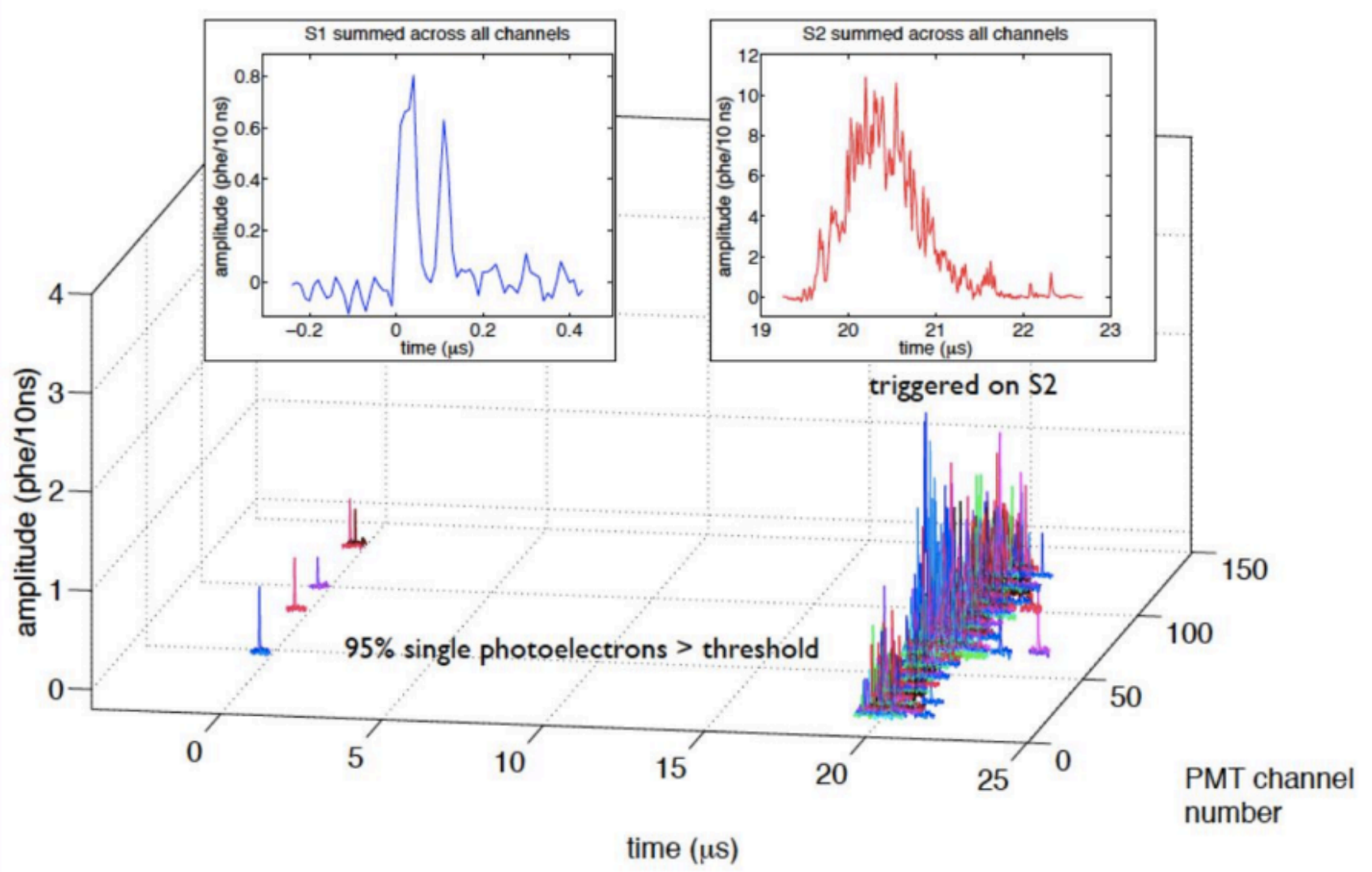

The Large Underground Xenon Experiment

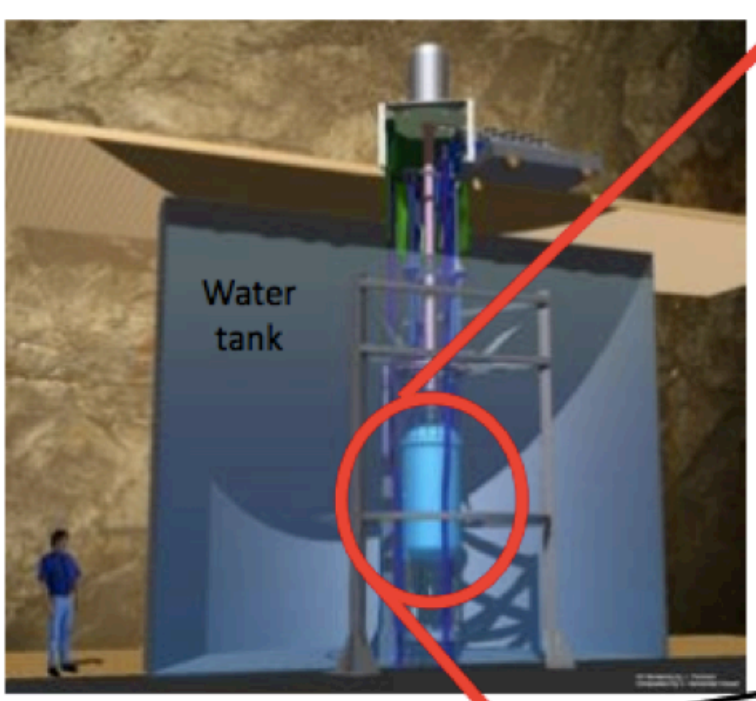

Low-radioactivity
Titanium Cryostat

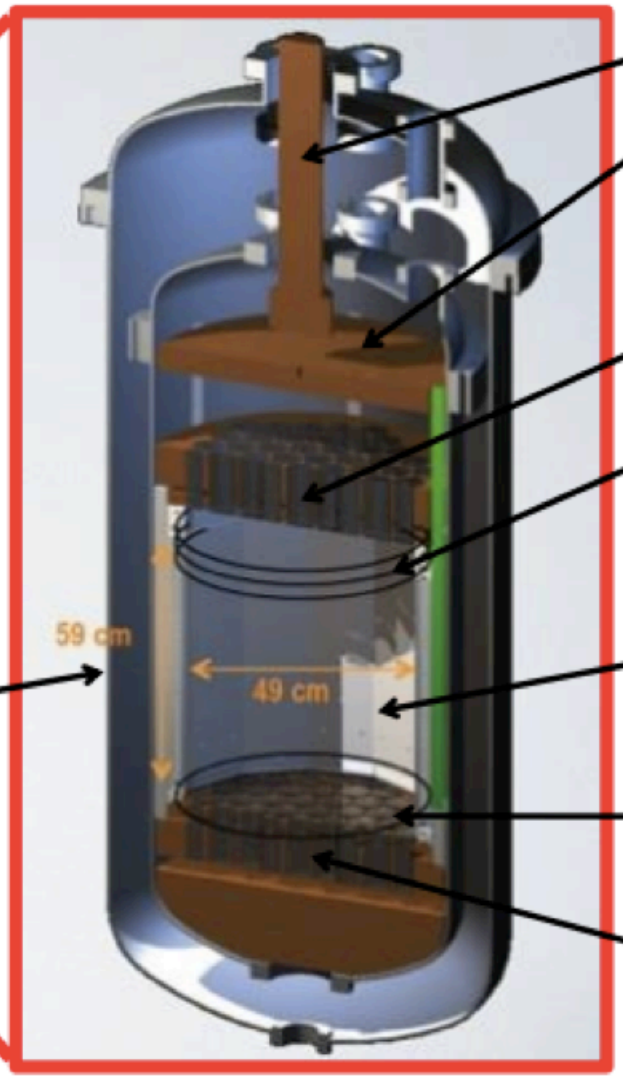

Thermosyphon

Copper shield

Top PMT array

Anode grid

PTFE reflector
panels and field
cage

Cathode grid

Bottom PMT array

370 kg total xenon mass
250 kg active liquid xenon
118 kg fiducial mass

The Large Underground Xenon Experiment

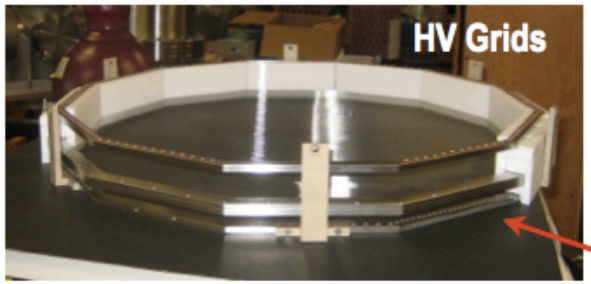

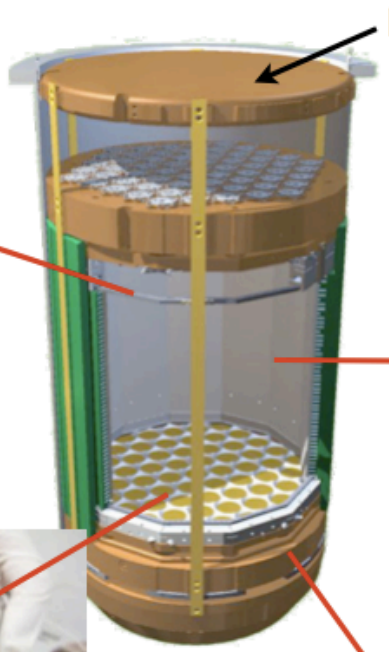

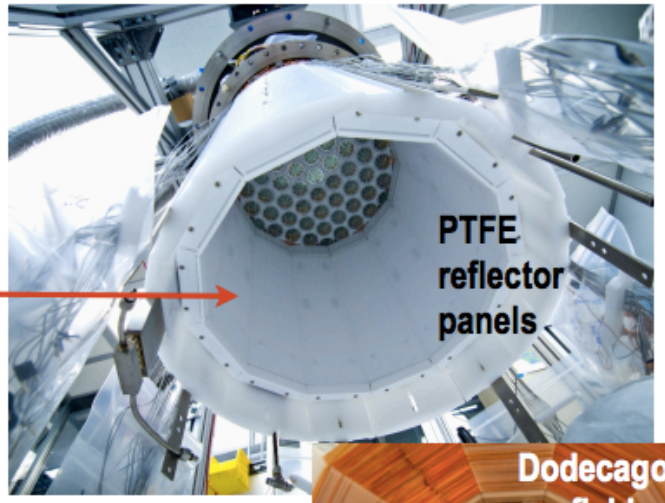

122 2" PMTs (Hamamatsu R8778)

- QE (175 nm) ~33%
- U/Th ~9/3 mBq/PMT

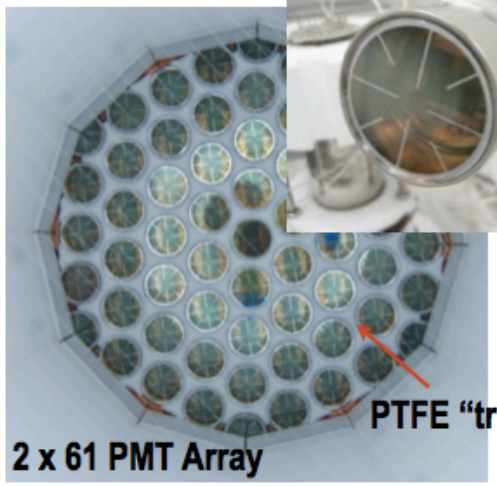

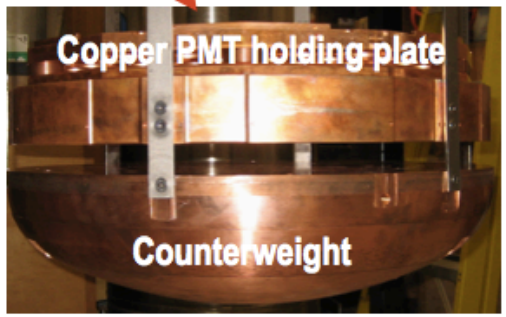

LUX First Underground Run - Overview

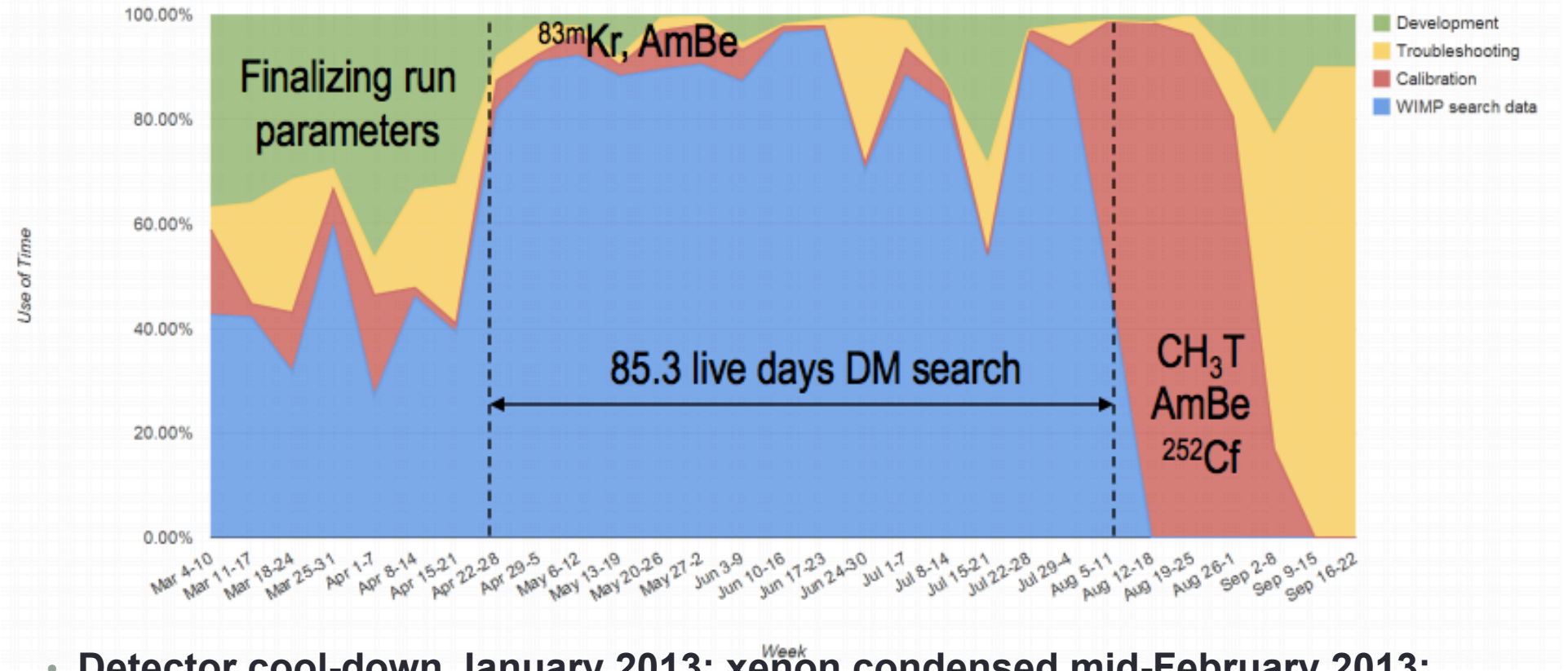

- **Detector cool-down January 2013; xenon condensed mid-February 2013; WIMP-search data collected from April to August 2013.**
- **Overall 95% data-taking efficiency during the WIMP search period**
- **Total: 85.3 live-days of WIMP-search data collected**

LUX First Underground Run - Parameters

- Xenon purity: electron drift length 87-135 cm
  - Continuous circulation at 250 kg/day through an external purifier
  - Monitored weekly using ^{83m}Kr injections
- Drift field: 181 V/cm (speed 1.5 mm/μs) with 99.6% ER discrimination
- Light collection efficiency: 14% (includes detector geometry and PMT QE; 3D corrections provided by ^{83m}Kr calibrations)
- NR calibrations with external AmBe and ^{252}Cf sources
- Precision ER calibrations performed with CH_3T injections after the WIMP-search campaign
- Fiducial mass: 118.3 +/- 6.5 kg
- WIMP-search window: ~3-25 keVnr

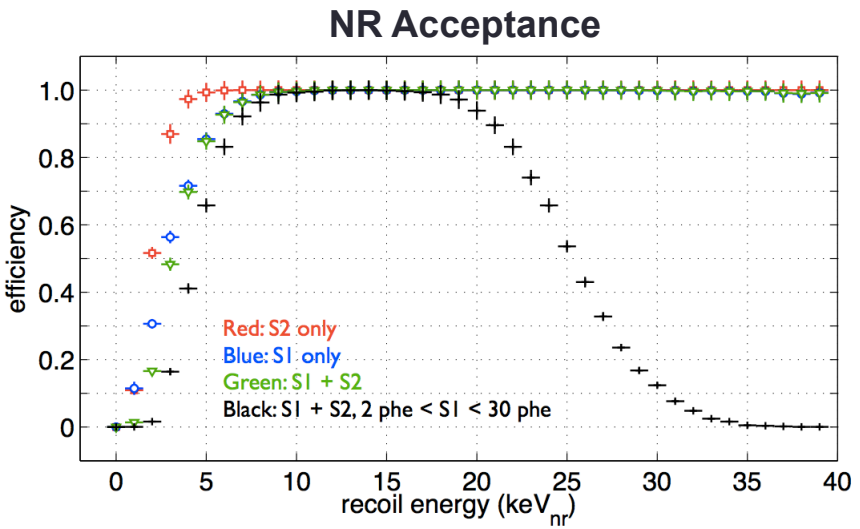

Event Selection and Cuts

Cut	Explanation	Events Remaining
All Triggers	S2 Trigger >99% for $S2_{raw}$>200 phe	83,673,413
Detector Stability	Cut periods of excursion for Xe Gas Pressure, Xe Liquid Level, Grid Voltages	82,918,901
Single Scatter Events	Identification of S1 and S2. Single Scatter cut.	6,585,686
S1 energy	Accept 2-30 phe (energy ~ 0.9-5.3 keVee, ~3-18 keVnr)	26,824
S2 energy	Accept 200-3300 phe (>8 extracted electrons) Removes single electron / small S2 edge events	20,989
S2 Single Electron Quiet Cut	Cut if >100 phe outside S1+S2 identified +/-0.5 ms around trigger (0.8% drop in livetime)	19,796
Drift Time Cut away from grids	Cutting away from cathode and gate regions, 60 < drift time < 324 us	8731
Fiducial Volume radius and drift cut	Radius < 18 cm, 38 < drift time < 305 us, 118 kg fiducial	160

Only simple, obvious cuts – no tuning beyond selecting a threshold, higher energy cutoff, and fiducial volume.

The LUX First WIMP-Search Result

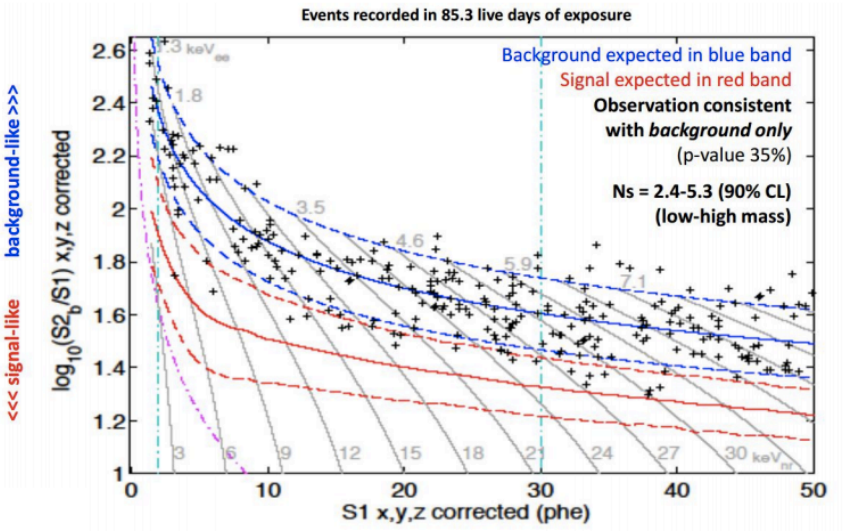

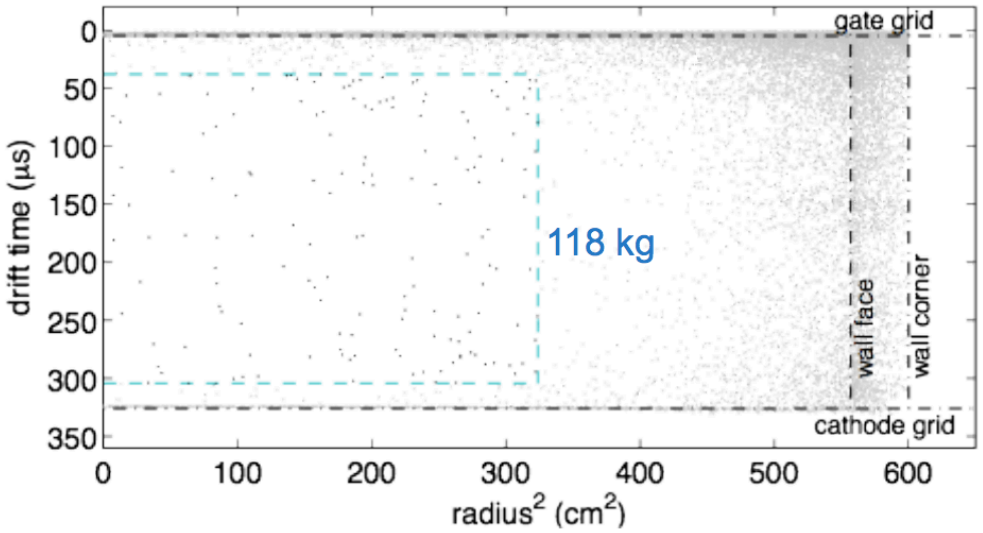

- **After all selection cuts, 160 candidate events left in the fiducial volume**
- **Distribution is consistent with electron recoil background and no WIMP signal with a p-value of 0.35 from Profile-Likelihood Ratio Analysis with incorporated background models, detector effects, and efficiencies**

The LUX First WIMP-Search Result And Beyond...

- **To date, LUX has set the setting the world's best limit on spin-independent WIMP-nucleon elastic scattering cross section:**

  7.6×10^{-46} cm^2 for 33 GeV-WIMPs

- **Since the end of the first run:**
  - **New NR calibration using a beam of mono-energetic neutrons from DD source => improved sensitivity at low masses**
  - **Currently: re-analysis taking place with improved low energy threshold**
- **300-live-day run to take place in 2015**
  - **Extending sensitivity by a factor of ~5**
  - **Discovery still possible!**

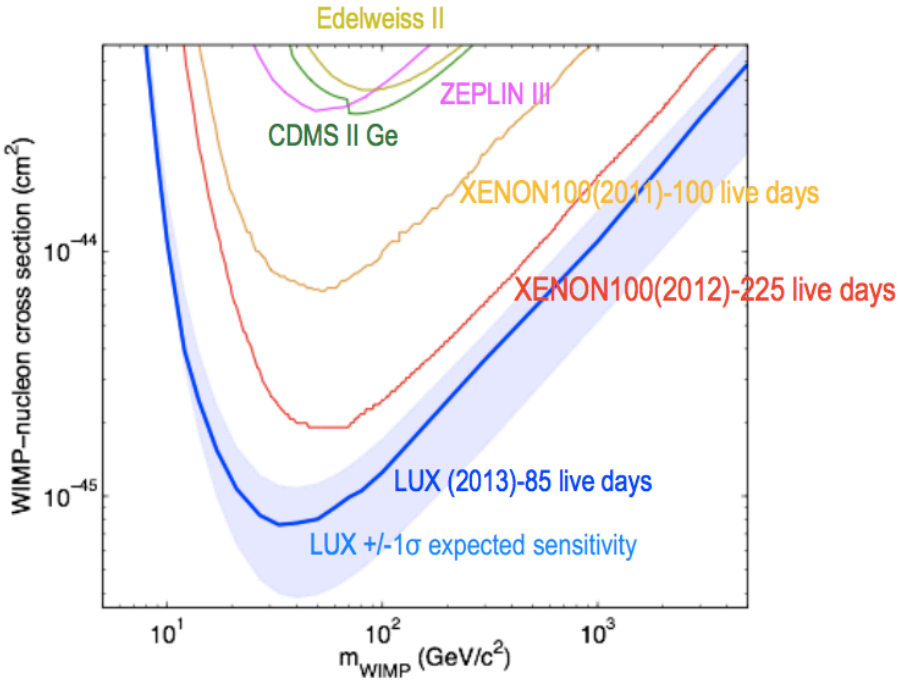

LUX 2013 result: PRL.112.091303 (arXiv:1310.8214)

Direct Detection Revisited

- **Direct detection experiments either:**
  - **Detect no excess of events, then use the energy spectrum predicted by a specific model of a specific interaction to set a limit on that particular interaction.**
  - **Detect an excess of events, in which case it is necessary to find a model that fits the observation.**
- **Direct detection experiments like LUX typically only work with two interaction models: spin-independent (SI) and spin-dependent (SD) elastic scattering interactions.**
  - **Comes from the assumption that momentum transfers involved in WIMP-nucleus scatters are nonrelativistic.**
  - **SI, SD interactions are the only interactions that do not vanish in the zero-momentum-transfer limit.**

Direct Detection Revisited

But there are several momentum- and velocity-dependent interactions also allowed by basic symmetry considerations.

- **The usual SI and SD interactions could be suppressed.**
- **Momentum transfer is not necessarily small on a parton scale.**
- **Novel nuclear responses such as angular-momentum-dependent (LD) and angular-momentum/spin-dependent (LSD) responses are allowed.**
- **These LD and LSD responses can interfere with the SI and SD responses.**

References: Fitzpatrick et al. arXiv:1203.3542 and arXiv:1211.2818
Anand et al. arXiv: 1308.6288 and arXiv:1405.6690
Cirelli et al. arXiv:1307.5955

Three Goals:

GOAL 1: Investigate the extent to which momentum/velocity-dependent interactions affect our signal in xenon.

GOAL 2: For a given target material (xenon), optimize analysis techniques to best probe these momentum/velocity-dependent interactions.

GOAL 3: (General) Check that the array of direct detection target materials currently in use do not leave any "blind spots" in WIMP parameter space.

The Effective Field Theory Setup

- **WIMP-nucleon elastic scattering is analogous to a four-fermion contact interaction in standard weak interaction theory.**

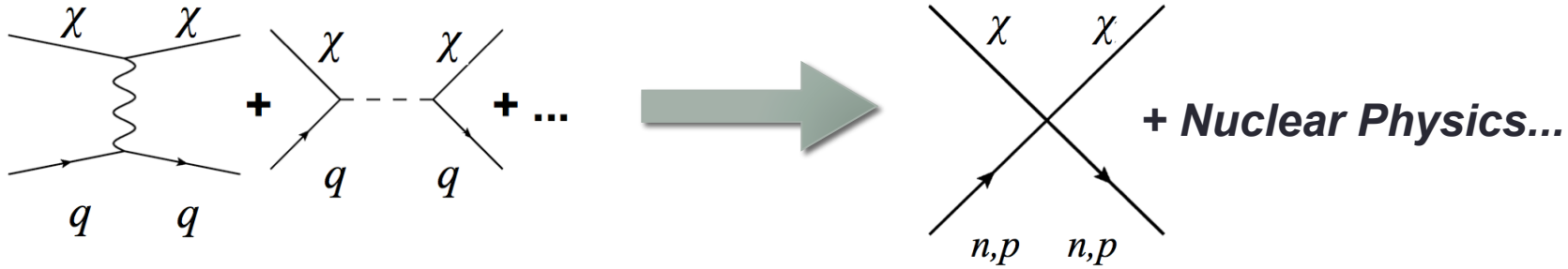

- **The general interaction Lagrangian:**

$$\mathcal{L}_{\rm int} = c\ \Psi_\chi^* \mathcal{O}_\chi \Psi_\chi\ \Psi_N^*\ \mathcal{O}_N \Psi_N = \sum_{i=1}^{\mathcal{N}} \left(c_i^{(n)} \mathcal{O}_i^{(n)} + c_i^{(p)} \mathcal{O}_i^{(p)} \right)$$

- **Restrict to operators O_i that are Galilean-invariant and Hermitian.**
- **Remaining O_i's are combinations of WIMP spin S_χ, nucleon spin S_N, incident velocity v^2, and momentum transfer q^2.**
- **Allow the O_i's to be at most quadratic in v (i.e. restrict to exchange of a spin-0 or spin-1 boson) and q (absorb higher powers of q into form factors).**

The Set of Allowed EFT Operators

SI Interaction

Cannot obtain at lowest order

SD Interaction

$$\mathcal{O}_1 = 1_\chi 1_N$$
$$\mathcal{O}_2 = (v^\perp)^2$$
$$\mathcal{O}_3 = i\vec{S}_N \cdot \left(\frac{\vec{q}}{m_N} \times \vec{v}^\perp\right)$$
$$\mathcal{O}_4 = \vec{S}_\chi \cdot \vec{S}_N$$
$$\mathcal{O}_5 = i\vec{S}_\chi \cdot \left(\frac{\vec{q}}{m_N} \times \vec{v}^\perp\right)$$
$$\mathcal{O}_6 = \left(\vec{S}_\chi \cdot \frac{\vec{q}}{m_N}\right)\left(\vec{S}_N \cdot \frac{\vec{q}}{m_N}\right)$$
$$\mathcal{O}_7 = \vec{S}_N \cdot \vec{v}^\perp$$
$$\mathcal{O}_8 = \vec{S}_\chi \cdot \vec{v}^\perp$$
$$\mathcal{O}_9 = i\vec{S}_\chi \cdot \left(\vec{S}_N \times \frac{\vec{q}}{m_N}\right)$$
$$\mathcal{O}_{10} = i\vec{S}_N \cdot \frac{\vec{q}}{m_N}$$
$$\mathcal{O}_{11} = i\vec{S}_\chi \cdot \frac{\vec{q}}{m_N}$$

- **Each nuclear form factor F_{ij} associated with the EFT operators can be written as a linear combination of five macroscopic nuclear responses that depend only on the nuclear physics: (arXiv:1203.3542)**

M	Σ'	Σ''	Δ	Φ''
SI response	SD response (longitudinal component)	SD response (transverse component)	LD (angular-momentum-dependent) response	LSD (spin-orbit) response

Converting Between the EFT Operators and the Macroscopic Nuclear Responses

	M (SI)	Σ'' (SD long.)	Σ' (SD trans.)	Δ (LD)	Φ'' (LSD)
O_1	q-indep.				
O_3			$\sim q^4, q^2v^2$		$\sim q^4$
O_4		q-indep.	q-indep.		
O_5	$\sim q^4, q^2v^2$			$\sim q^4$	
O_6		$\sim q^4$			
O_7			$\sim q^2, v^2$		
O_8	$\sim q^2, v^2$			$\sim q^2$	
O_9			$\sim q^2$		
O_{10}		$\sim q^2$			
O_{11}	$\sim q^2$				

Comparing Target Materials

- **Estimate the number of predicted events as:**

$$\frac{dN}{dE_R} \sim 5000\text{keV}^{-1} \left(\frac{\text{exposure}}{\text{kg}\cdot\text{day}}\right) \left(\frac{100\text{GeV}}{m_\chi}\right)^3 \mathcal{L}^2_{\text{int}}$$

- **Comparing the interaction terms for different targets:**

	S_n^2	S_p^2	L_n^2	L_p^2	$(S_n \cdot L_n)^2$	$(S_p \cdot L_p)^2$
F	$8 \cdot 10^{-5}$	0.2	0.04	0.05	0.6	0.1
Na	0.0004	0.06	0.1	0.8	5.5	3.3
Ge	0.02	$5 \cdot 10^{-6}$	1.1	0.003	35	100
I	0.004	0.07	0.4	2.	100	500
Xe	0.02	$2 \cdot 10^{-5}$	0.4	0.04	500	300

(arXiv:1211.2818)

- **Xenon is sensitive to not only SD WIMP-neutron interactions, but also to the new LD (Δ) and LSD (Φ'') interactions for both nucleons.**

SI and LD WIMP-n Recoil Spectra

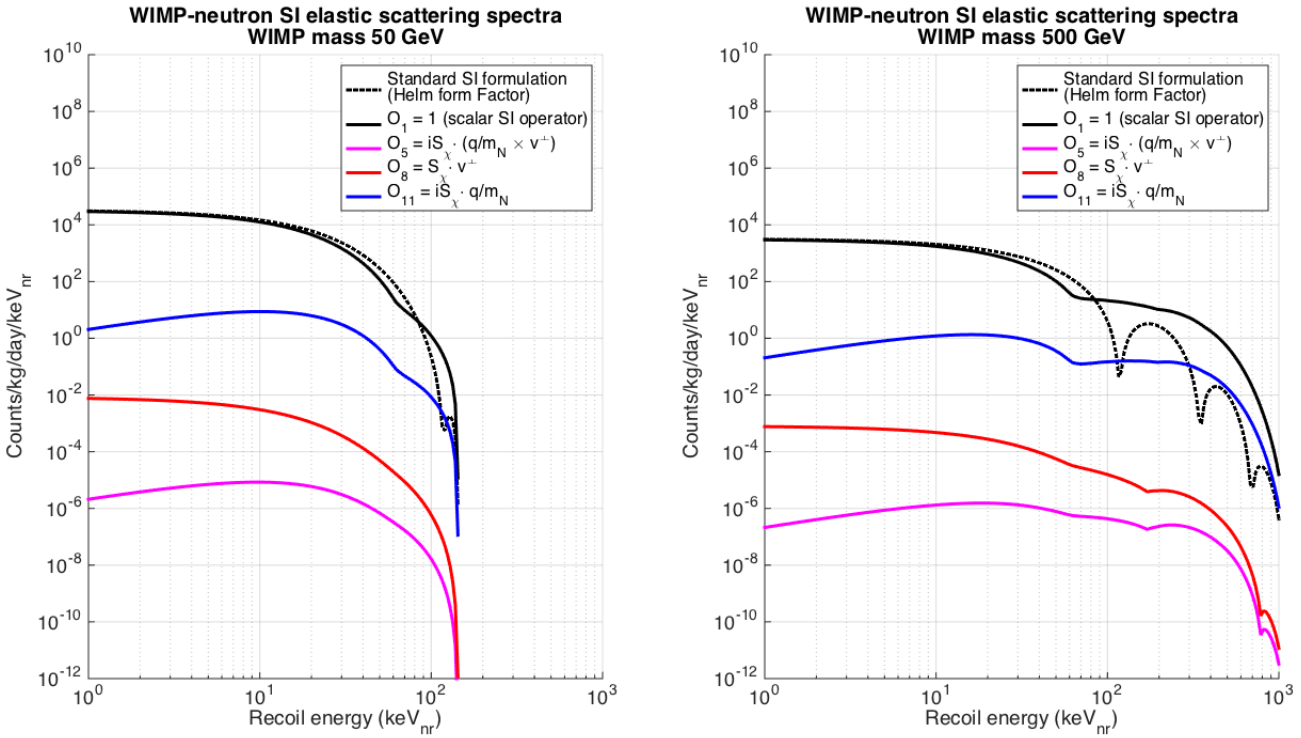

- **A note on normalization of spectra: Note that the usual WIMP-nucleon cross section σ_0 refers to "cross section at zero-momentum-transfer". This only makes sense for the usual SI and SD interactions.**
  - **All coupling constants C_i normalized to each other.**
  - **C_1 chosen to correspond to σ_0 = 1 pb**

SI and LD WIMP-n Recoil Spectra

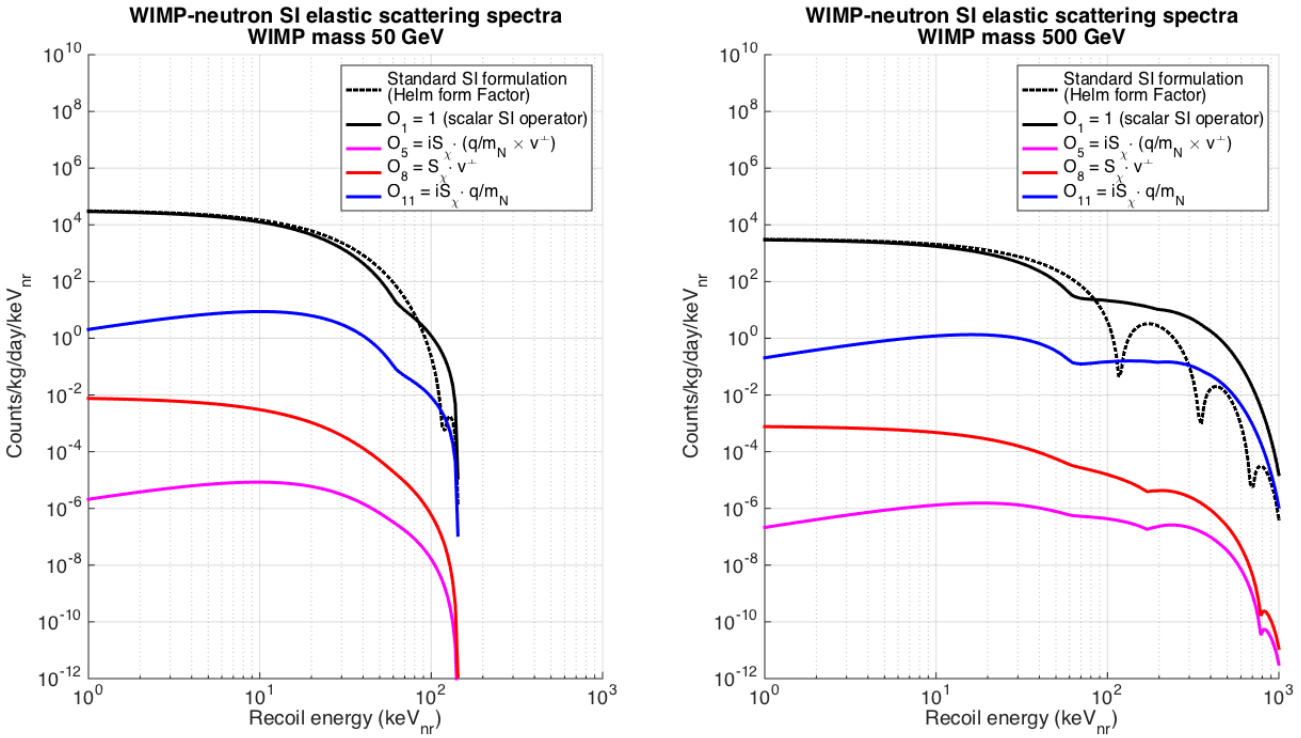

- O_1 (the usual SI interaction) and O_{11} both produce an SI response, but the spectra have different slopes due to different *q*-dependence.
- O_5 and O_8 each produce both an LD and an SI response, again with different *q*-dependence.
- For m_{WIMP} large, the EFT spectra stay relatively flat out to ~few hundred keV.

SI and LD WIMP-n Integrated Spectra

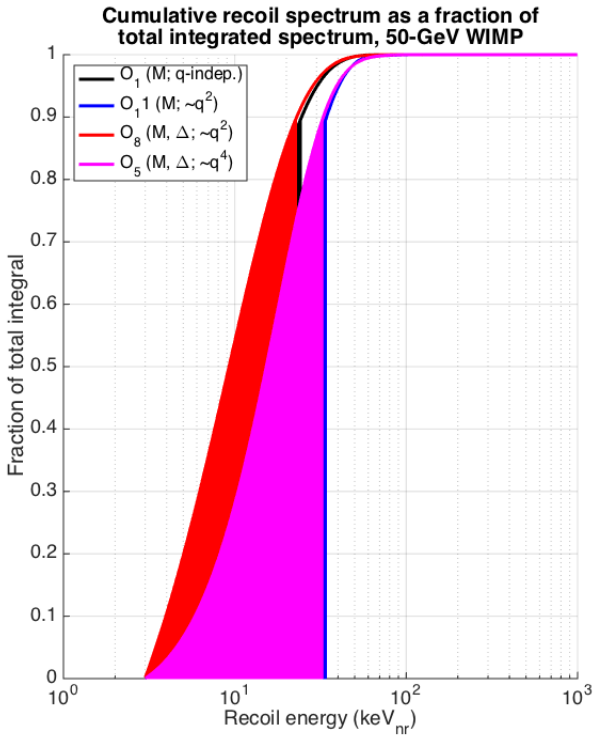

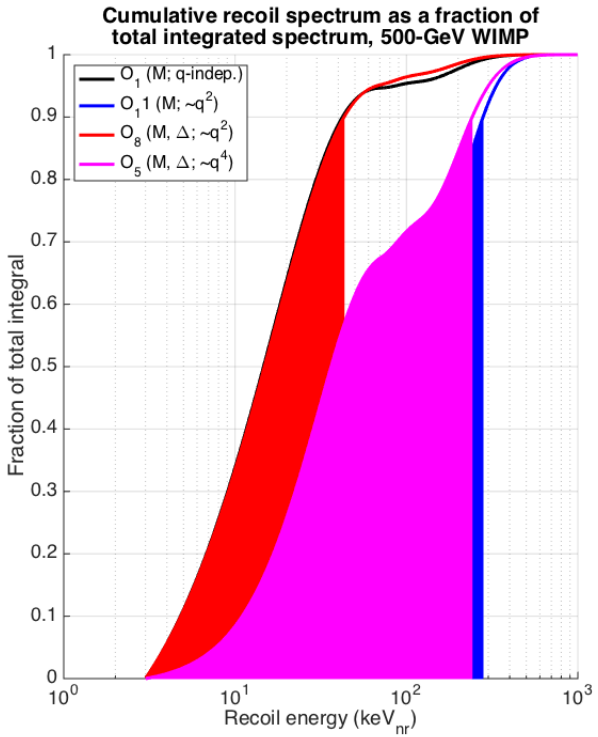

- **Integrating under each of the spectra, we find that in order to capture 90% of the signal, we require an upper energy threshold of up to ~40 keV for 50-GeV WIMPs and up to ~300 keV for 500-GeV WIMPs.**

SD and LSD WIMP-n Recoil Spectra

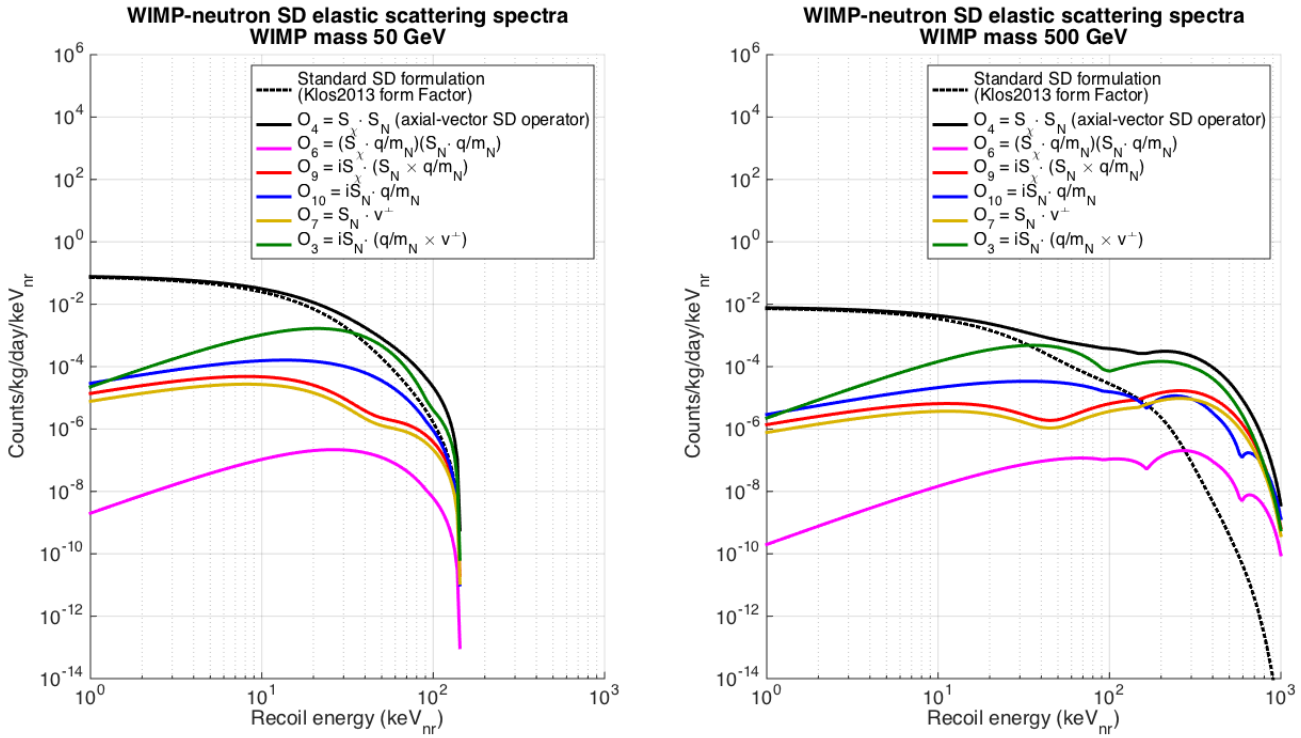

- **The two types of SD response (transverse and longitudinal to the momentum transfer *q*) exhibit distinctly different behaviors.**
- **Again the slope of the spectrum depends on the *q*-dependence of the operator.**
- **O_3 (green) is the only LSD operator. Its spectrum increases sharply to around 50 keV and does not begin to decrease until ~300 keV for heavy WIMPs.**

SD and LSD WIMP-n Integrated Spectra

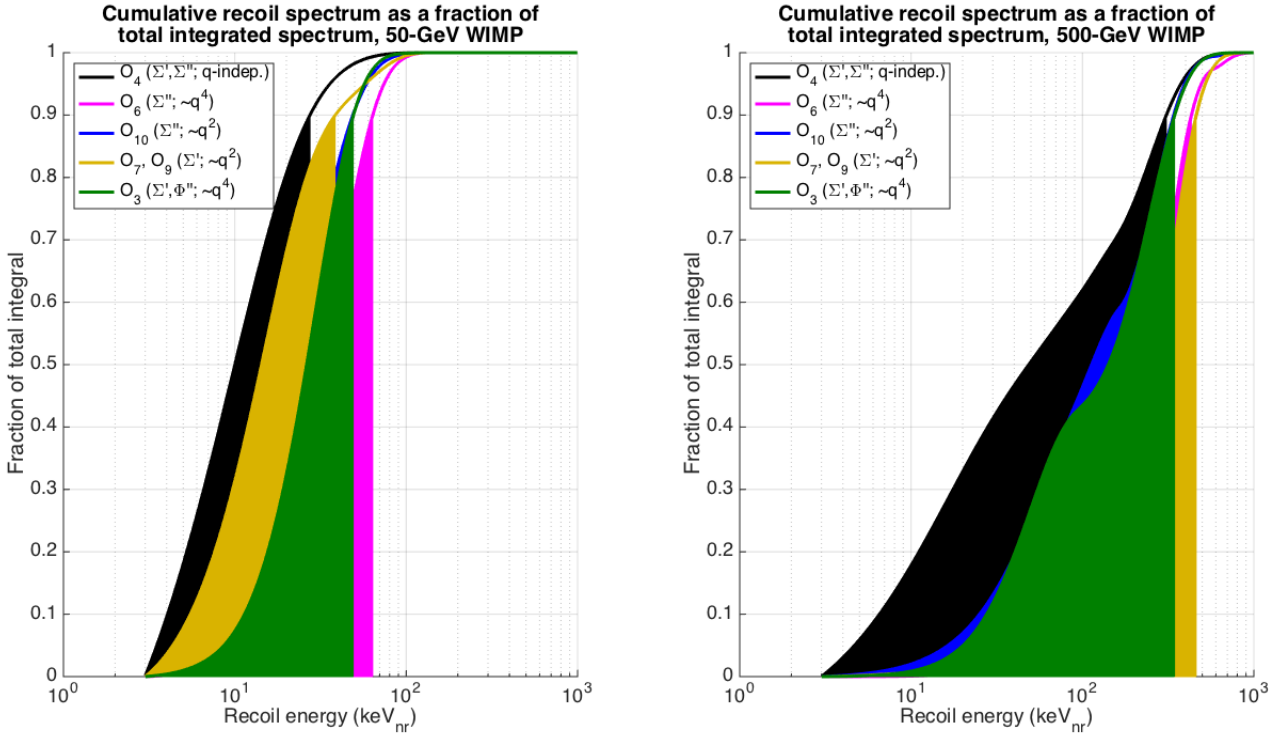

- **Integrating under the spectra, we again find that in order to capture 90% of the prospective signal we require a WIMP-search window that goes up to ~60 keV for a 50-GeV WIMP and several hundred keV for a 500-GeV WIMP.**
- **Holds true for essentially all the operators.**

Optimizing the WIMP-Search Window

Table: The minimum upper bound on the WIMP-search window in keVnr for the WIMP-search region to contain 50% or 90% of the integrated spectrum

	Operator	50-GeV WIMP		500-GeV WIMP	
		50%	90%	50%	90%
SI	Standard SI	10.8	27.3	16.6	44.7
	O_1	9.9	24.6	14.7	42.4
	O_{11}	16.4	34.4	39.8	281
SI + LD	O_5	15.3	32.8	36.5	243
	O_8	9.3	23.0	14.9	43.4
SD	Standard SD	8.6	21.6	11.9	37.5
	O_4	10.0	27.6	48.8	310
	O_6	33.6	64.1	268	434
	O_9	14.4	38.6	277	463
	O_{10}	22.2	49.0	113	342
	O_7	14.4	38.6	277	463
SD + LSD	O_3	26.3	49.2	142	346

For many of the new momentum-dependent operators, we require a search window of up to several hundred keVnr to capture most of the signal.

Constraints on Representative Operators

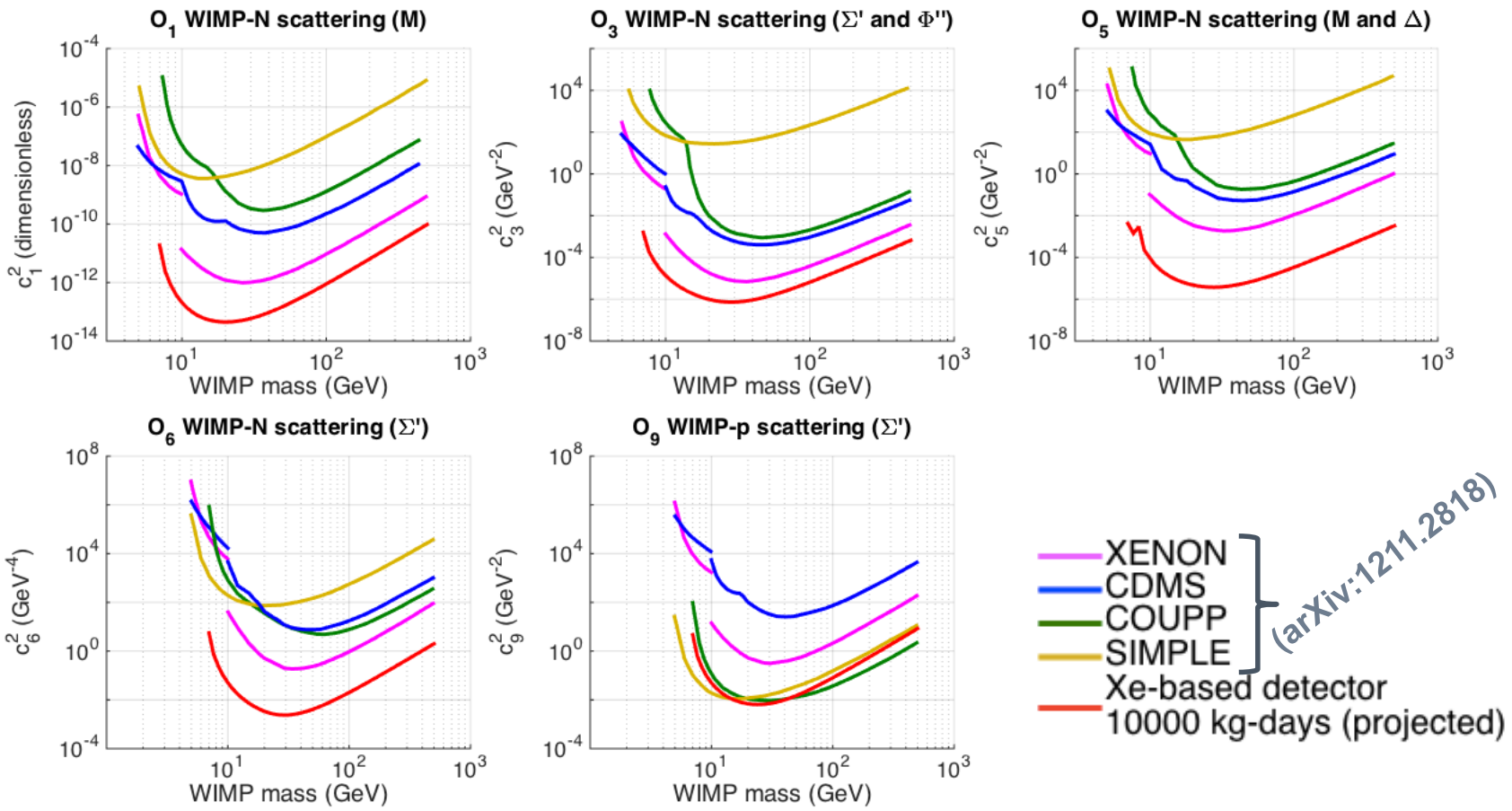

Constraints on Representative Operators

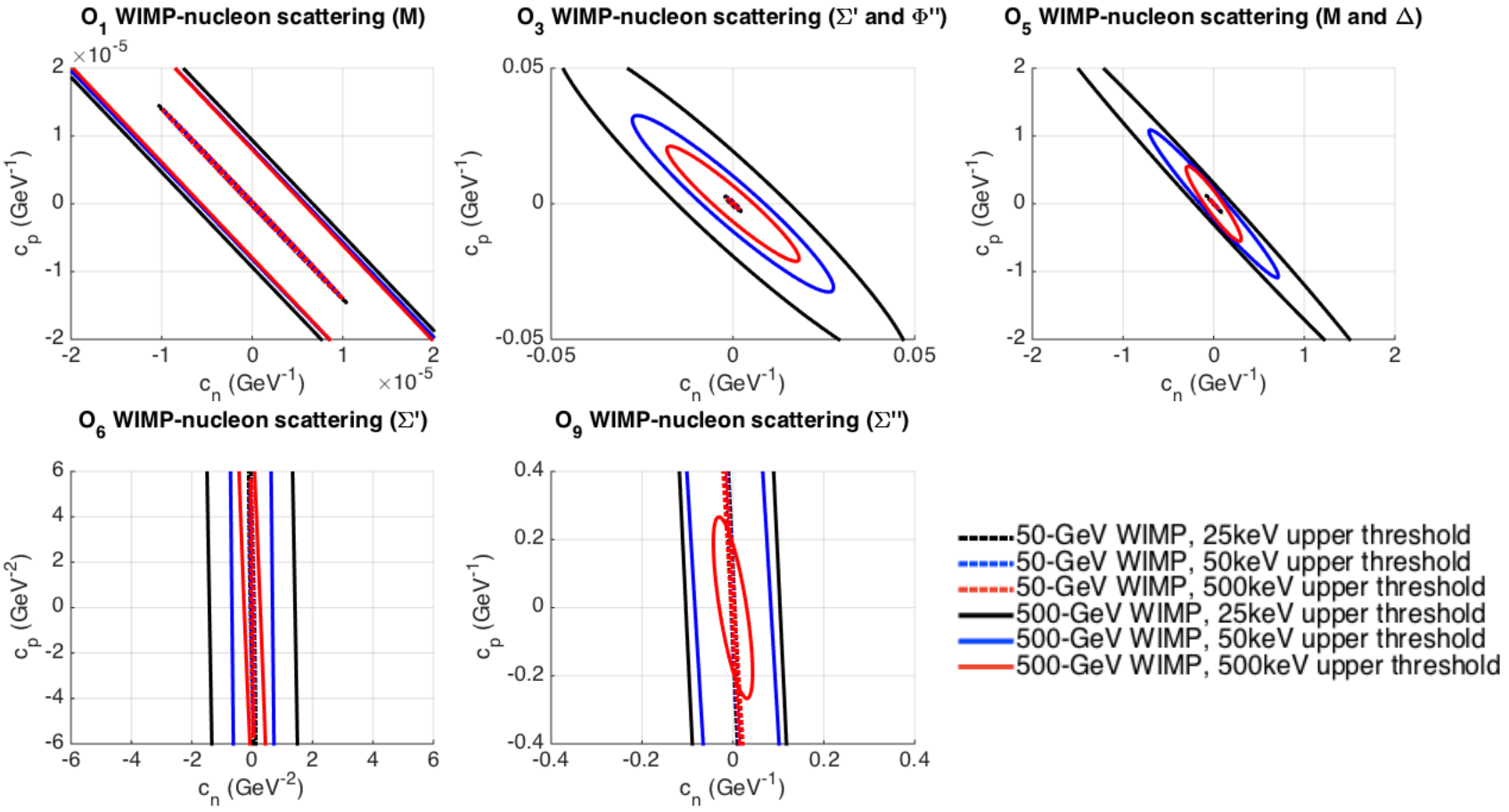

All exclusion curves shown are for a xenon target with 10000 kg-day exposure.

Summary

- **Direct detection experiments traditionally only present limits on interactions that vanish in the zero-momentum-transfer limit (SI and SD).**
  - **There is at least one additional momentum-dependent interaction (O_{11}) that can produce a spin-independent nuclear response.**
  - **There are at least four additional momentum-and-velocity-dependent interactions (O_6, O_9, O_{10}, O_7) that can produce a spin-dependent nuclear response, with transverse and longitudinal components of the spin-dependent response showing distinctly different behaviors.**
  - **There are two additional operators that produce an entirely new angular-momentum-dependent nuclear response (O_5, O_8) in addition to producing an SI response.**
  - **There is one additional operator that produces an entirely new angular-momentum-and-spin-dependent nuclear response (O_3) in addition to producing an SD response.**

Xenon is sensitive to these new interactions but the bulk of the signal lies well above the 3-25 keVnr WIMP-search window used by LUX and other experiments.

Current Status and Next Steps

- **Current status: Spectra have been generated and simple cut-and-count limits produced for each of the new operators for a xenon target.**
- **Short-term: Generate signal models using these EFT spectra and run them through the LUX PLR to produce limits on each of the new operators using the WIMP-search data from the LUX first underground run.**
- **Next, increase the upper threshold of the WIMP-search window from ~25 keVnr to ~few hundred keVnr.**
  - **This will allow us to better optimize signal-to-background based on where the spectrum peaks for each of the momentum/velocity-dependent EFT operators.**
- **At higher recoil energies pulse-shape cuts and other discrimination techniques can be used to help with signal-to-noise ratio.**

Thank you!

Brown

Richard Gaitskell	PI, Professor
Simon Fiorucci	Research Associate
Monica Pangilinan	Postdoc
Jeremy Chapman	Graduate Student
David Malling	Graduate Student
James Verbus	Graduate Student
Samuel Chung Chan	Graduate Student
Dongqing Huang	Graduate Student

Case Western

Thomas Shutt	PI, Professor
Dan Akerib	PI, Professor
Karen Gibson	Postdoc
Tomasz Biesiadzinski	Postdoc
Wing H To	Postdoc
Adam Bradley	Graduate Student
Patrick Phelps	Graduate Student
Chang Lee	Graduate Student
Kati Pech	Graduate Student

Imperial College London

Henrique Araujo	PI, Reader
Tim Sumner	Professor
Alastair Currie	Postdoc
Adam Bailey	Graduate Student

Lawrence Berkeley + UC Berkeley

Bob Jacobsen	PI, Professor
Murdock Gilchriese	Senior Scientist
Kevin Lesko	Senior Scientist
Carlos Hernandez Faham	Postdoc
Victor Gehman	Scientist
Mia Ihm	Graduate Student

Lawrence Livermore

Adam Bernstein	PI, Leader of Adv. Detectors Group
Dennis Carr	Mechanical Technician
Kareem Kazkaz	Staff Physicist
Peter Sorensen	Staff Physicist
John Bower	Engineer

LIP Coimbra

Isabel Lopes	PI, Professor
Jose Pinto da Cunha	Assistant Professor
Vladimir Solovov	Senior Researcher
Luiz de Viveiros	Postdoc
Alexander Lindote	Postdoc
Francisco Neves	Postdoc
Claudio Silva	Postdoc

SD School of Mines

Xinhua Bai	PI, Professor
Tyler Liebsch	Graduate Student
Doug Tiedt	Graduate Student

SDSTA

David Taylor	Project Engineer
Mark Hanhardt	Support Scientist

Texas A&M

James White †	PI, Professor
Robert Webb	PI, Professor
Rachel Mannino	Graduate Student
Clement Sofka	Graduate Student

UC Davis

Mani Tripathi	PI, Professor
Bob Svoboda	Professor
Richard Lander	Professor
Britt Holbrook	Senior Engineer
John Thomson	Senior Machinist
Ray Gerhard	Electronics Engineer
Aaron Manalaysay	Postdoc
Matthew Szydagis	Postdoc
Richard Ott	Postdoc
Jeremy Mock	Graduate Student
James Morad	Graduate Student
Nick Walsh	Graduate Student
Michael Woods	Graduate Student
Sergey Uvarov	Graduate Student
Brian Lenardo	Graduate Student

UC Santa Barbara

Harry Nelson	PI, Professor
Mike Witherell	Professor
Dean White	Engineer
Susanne Kyre	Engineer
Carmen Carmona	Postdoc
Curt Nehrkorn	Graduate Student
Scott Haselschwardt	Graduate Student

University College London

Chamkaur Ghag	PI, Lecturer
Lea Reichhart	Postdoc

University of Edinburgh

Alex Murphy	PI, Reader
Paolo Beltrame	Research Fellow
James Dobson	Postdoc

University of Maryland

Carter Hall	PI, Professor
Attila Dobi	Graduate Student
Richard Knoche	Graduate Student
Jon Balajthy	Graduate Student

University of Rochester

Frank Wolfs	PI, Professor
Wojtek Skutski	Senior Scientist
Eryk Druszkiewicz	Graduate Student
Mongkol Moongweluwan	Graduate Student

University of South Dakota

Dongming Mei	PI, Professor
Chao Zhang	Postdoc
Angela Chiller	Graduate Student
Chris Chiller	Graduate Student
Dana Byram	*Now at SDSTA

Yale

Daniel McKinsey	PI, Professor
Peter Parker	Professor
Sidney Cahn	Lecturer/Research Scientist
Ethan Bernard	Postdoc
Markus Horn	Postdoc
Blair Edwards	Postdoc
Scott Hertel	Postdoc
Kevin O'Sullivan	Postdoc
Nicole Larsen	Graduate Student
Evan Pease	Graduate Student
Brian Tennyson	Graduate Student
Ariana Hackenburg	Graduate Student
Elizabeth Boulton	Graduate Student

Extra Slides